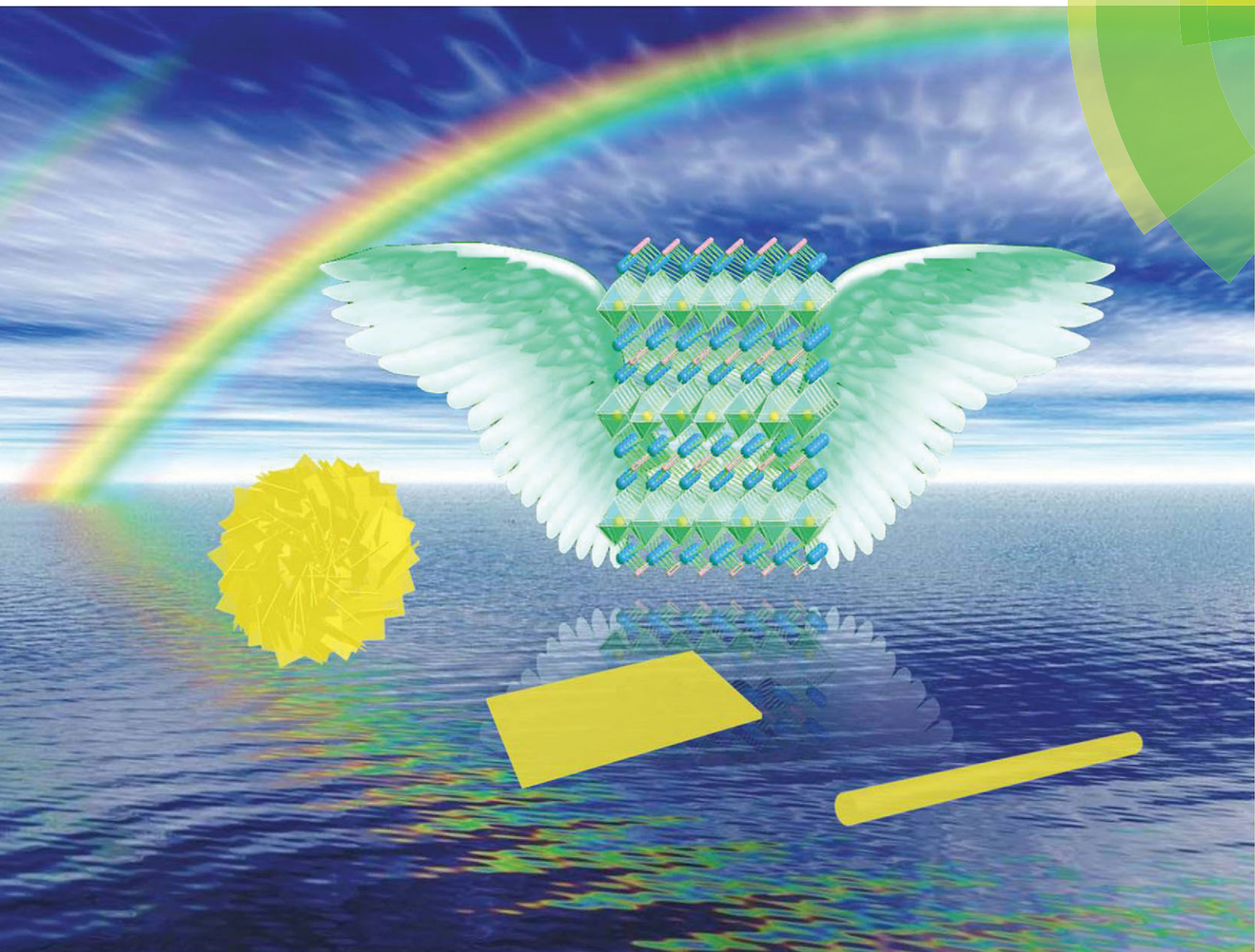


Chem Soc Rev

Chemical Society Reviews

www.rsc.org/chemsocrev



ISSN 0306-0012



REVIEW ARTICLE

Mario Pagliaro, Yi-Jun Xu *et al.*

Nanochemistry-derived Bi_2WO_6 nanostructures: towards production of sustainable chemicals and fuels induced by visible light

Nanochemistry-derived Bi₂WO₆ nanostructures: towards production of sustainable chemicals and fuels induced by visible light

Cite this: *Chem. Soc. Rev.*, 2014, 43, 5276

Nan Zhang,^{ab} Rosaria Ciriminna,^c Mario Pagliaro*^c and Yi-Jun Xu*^{ab}

Low cost and easily made bismuth tungstate (Bi₂WO₆) could be one of the key technologies to make chemicals and fuels from biomass, atmospheric carbon dioxide and water at low cost using solar radiation as an energy source. Its narrow band gap (2.8 eV) enables ideal visible light ($\lambda > 400$ nm) absorption. Yet, it is the material's shape, namely the superstructure morphology wisely created *via* a nanochemistry approach, which leads to better electron–hole separation and much higher photoactivity. Recent results coupled to the versatile photochemistry of this readily available semiconductor suggest that the practical application of nanochemistry-derived Bi₂WO₆ nanostructures for the synthesis of value-added fine chemicals and fuel production is possible. We describe progress in this important field of chemical research from a nanochemistry viewpoint, and identify opportunities for further progress.

Received 31st January 2014

DOI: 10.1039/c4cs00056k

www.rsc.org/csr

1. Introduction

In a famous lecture¹ at the International Congress of Applied Chemistry held in 1912, Giacomo Ciamician forecasted the future production of fuels and chemicals by means of artificial photosynthesis using the immense amount of solar energy received by the Earth each day, in place of utilising “fossil solar

energy” (coal and oil, at that time; and also natural gas since the late 1950s). Production of fuels and chemicals through solar energy, water and biomass, however, thus far has remained largely untapped. Only recently – thanks to sol-gel bioreactors² in which the entrapped cells are alive after one year with constant photosynthetic activity – has this ultimate objective of chemical research commenced to achieve yields and photosynthetic stability levels worth to be taken into consideration from a practical viewpoint.

Continuing to burn coal and hydrocarbons, the global carbon dioxide emissions in the atmosphere have grown to a record high of 35.6 billion tons in 2012,³ not to mention the pollution problems related to the emissions of noxious substances including Hg derived from burning coal and methane.

^a State Key Laboratory of Photocatalysis on Energy and Environment, College of Chemistry, Fuzhou University, Fuzhou 350002, P.R. China.

E-mail: yjxu@fzu.edu.cn; Fax: +86 591 83779326; Tel: +86 591 83779326

^b College of Chemistry, New Campus, Fuzhou University, Fuzhou 350108, P.R. China

^c Istituto per lo Studio dei Materiali Nanostrutturati, CNR, via U. La Malfa 153, 90146 Palermo, Italy. E-mail: mario.pagliaro@cnr.it



Nan Zhang

Nan Zhang is currently a PhD student in Professor Yi-Jun Xu's group at State Key Laboratory of Photocatalysis on Energy and Environment at Fuzhou University, P.R. China. Her main research interests include the fabrication of core-shell and carbon-based nanocomposites for potential target applications in heterogeneous photocatalysis. She has coauthored more than 30 papers on the topics of her research.



Rosaria Ciriminna

Rosaria Ciriminna is a frequently cited chemistry scholar based at Palermo's Institute of Nanostructured Materials of Italy's CNR. Her research on sustainability through nanochemistry has resulted in a number of achievements that currently find employment in new catalysts and sensors. She has coauthored more than 100 papers and several books on the topics of her research.

In short, one century after Ciamician's insight into "the photochemistry of the future",¹ we need to rapidly turn to solar energy for making useful energy (electricity and heat) and purposeful chemicals.

One good news is that today's low cost photovoltaics and solar thermal technologies have been impacting the way we create electricity and low temperature heat, with impressive growth figures recorded in wealthy as well as in developing countries. As a representative example, as of early 2014, the world's cumulative installed photovoltaic power exceeded 136 GW. In 2000, the overall PV solar power deployed across the world was 1.4 GW.

As early as 1972, Fujishima and Honda found that water can be split into O₂ and H₂ by irradiation of a single crystal TiO₂ anode connected with a Pt black cathode through an external load.⁴ Since then, a great deal of research has been devoted to semiconductor photocatalysis.^{5–13} Thanks to nearly four decades of efforts by several groups worldwide, today titania-based photocatalysis has been commercially employed for the oxidative degradation (mineralization) of pollutants mainly through adding photocatalytic titania in paints, photocatalytic concrete and ceramic tiles.¹⁴ Notably, such technology has not been applied commercially for organic synthesis or fuel production, even though some progress towards selective photosynthetic processes and fuel evolution using chemically doped titania has been achieved.^{8–12}

For a practical system, an energy efficiency of at least 10% is necessary,¹⁵ but the TiO₂-based cells can never attain the specified 10% level of solar-to-hydrogen conversion efficiency since with the large band gap semiconductor TiO₂ absorbs only ultraviolet photons ($\lambda < 400$ nm), which account for about 4% of the sunlight, leading to a photoconversion efficiency of less than 2.2% under air mass (AM) 1.5 solar illumination.¹⁶

Visible light contributes about 50% of solar radiation, and is freely and abundantly available across the globe. Considerable attention has therefore been paid to development of visible-light-active materials.^{17–29} Traditional visible-light photocatalysts include metal chalcogenides^{17–20} and binary metal oxides composed of transition metal cations with dⁿ or post-transition metal cations with ns² electronic configurations.^{23–29} However, the application of

metal chalcogenides (*e.g.*, CdS, CdSe, *etc.*) is significantly limited by their insufficient stability.^{19,20,30} Transition metal oxides (*e.g.*, Fe₂O₃, Co₃O₄, *etc.*) suffer from high resistivity due to the small polaron-dominated conductivity,^{27,31} which makes the photogenerated carrier extraction and transport difficult.^{32,33} As for post-transition metal oxides (*e.g.*, PbO, Bi₂O₃, *etc.*), although the post-transition metal cations possess occupied high binding energy s states, giving rise to an O 2p metal p narrow band gap,^{29,34} the coupling between the filled cation s and anion p states generally results in an unfavorable indirect band gap³⁵ (where band edge optical absorption varies with the square root of the photon energy).³⁶ This inevitably decreases the carrier extraction efficiencies. Some ultraviolet light-active oxides have been somehow turned into visible-light photocatalysts by substitutional doping with metal species, such as Ni_xIn_{1-x}TaO₄³⁷ and V-, Fe-, or Mn-TiO₂,³⁸ or with nonmetal elements, such as TiO_{2-x}C_x,^{39,40} TiO_{2-x}N_x,⁴¹ TiO_{2-x}S_x,⁴² and tantalum oxynitride.⁴³ Nevertheless, their activities are often low and there is concern for the stability of substituted ions under reaction conditions.^{37–43} Consequently, in order to overcome the intrinsic limitations of binary metal oxides for next generation photocatalytic applications, it is of great importance to combine multiple cations to form functionalized *ternary* oxides with appropriate properties and performance.

On the other hand, bearing the energy crisis in mind, research chemists must devise new efficient methods using solar radiation as an energy source to make chemicals from biomass in place of oil feedstock, and to produce fuels from water or excess atmospheric carbon dioxide obtained by fossil fuel combustion, to accumulate daily and seasonal intermittent solar energy. The progress in semiconductor-based photocatalytic selective organic transformations^{44–58} and solar water splitting^{59–65} highlights that the appropriate choice of semiconductors (*e.g.*, tuning the structure, morphology and interface composition) along with optimization of the process can impact these two objectives.

In this context, in 1999 Kudo and Hiji firstly synthesized ternary metal oxide direct semiconductor Bi₂WO₆ *via* conventional solid state reaction and utilized it for photocatalytic O₂ evolution under visible light irradiation.⁶⁶ Bi₂WO₆, as one of the simplest members of the Aurivillius family, is composed of



Mario Pagliaro

Mario Pagliaro is a chemistry and solar energy scholar at Italy's Research Council. His research and educational interests encompass a broad field from sol-gel functional materials through helionomics, a term he introduced in 2008. Mario chairs the SuNEC and FineCat international meetings held annually in Sicily since 2011.



Yi-Jun Xu

Yi-Jun Xu is a full professor now working at State Key Laboratory of Photocatalysis on Energy and Environment at Fuzhou University, P.R. China. His current research interests primarily focus on the assembly and application of semiconductor-based nano-structured materials, such as graphene-based and core-shell composite photocatalysts, in the field of heterogeneous photocatalysis.

perovskite-like $[\text{WO}_4]^{2-}$ layers sandwiched between bismuth oxide $[\text{Bi}_2\text{O}_2]^{2+}$ layers.^{67,68} Such structure favors the efficient separation of photogenerated electron–hole pairs and then improves the photocatalytic activity, which can be ascribed to the formed internal electric fields between the slabs.^{68,69} Due to its preferable band composition and unique layered structure, Bi_2WO_6 possesses several advantages as photocatalysts over the competing materials, especially in the view of practical applications, including its desirable visible light absorption, relatively high photocatalytic activity and good stability. Therefore, visible light-driven Bi_2WO_6 photocatalysts have attracted extensive research attention.^{68–101} Chemists discovered that nanostructured Bi_2WO_6 shows even more promising visible light photocatalytic activities.^{68–101} This was first demonstrated for the photocatalytic degradation of organics using Bi_2WO_6 nanosheets, nanofibers, hierarchical architectures and ordered arrays,^{68–76,78–80,84,86–91} and later on for fuel production from carbon dioxide and water using Bi_2WO_6 nanoplates, microspheres, inverse opals and films.^{94–98} Afterwards, the highly selective synthetic processes capable of affording value-added oxygenated chemicals from glycerol, an eminent biochemical platform,¹⁰² and alcohols were achieved over flower-like and silica-entrapped Bi_2WO_6 using oxygen as an oxidant in water under ultramild conditions.^{99–101}

Thus far, three reviews on Bi_2WO_6 photocatalysts have been published.^{68,70,71} All three focus on non-selective chemical processes, including the degradation of organic pollutants as well as the disinfection of bacteria.^{68,70,71} However, no single review summarizes achievements with this class of visible light photocatalysts in the promising field of selective organic transformations and fuel production, which are the critical focus of the present study.

In this account, we show how nanochemistry is actually used to make low-cost Bi_2WO_6 nanostructures that are efficient mediators for making highly active visible light photocatalysts for selective organic synthesis and fuel production, including aerobic oxidation of glycerol and alcohols,^{99–101} reduction of carbon dioxide to the fuels^{94,95} and water splitting for hydrogen evolution.^{96–98} The study is concluded by a discussion on practical aspects including results from recent applications of photocatalysis and issues of cost and materials availability, keeping a broad range of readers abreast of this significant current research fields, and casting a glance to the future perspective associated with Bi_2WO_6 nanostructure toward sustainable production of chemicals and fuels.

2. Bi_2WO_6 nanostructures

Bi_2WO_6 consists of accumulated layers of corner-sharing WO_6 octahedral sheets and bismuth oxide sheets.^{66,90} The conduction band (CB) of Bi_2WO_6 is composed of the $\text{W}5d$ orbital; its valence band (VB) is formed by the hybridization of the $\text{O}2p$ and $\text{Bi}6s$ orbitals, which not only makes the VB largely dispersed and thus results in a narrowed band gap of Bi_2WO_6 (2.8 eV) capable of absorbing visible light ($\lambda > 400$ nm), but also favors the mobility of photogenerated holes for specific oxidation reaction.⁷²

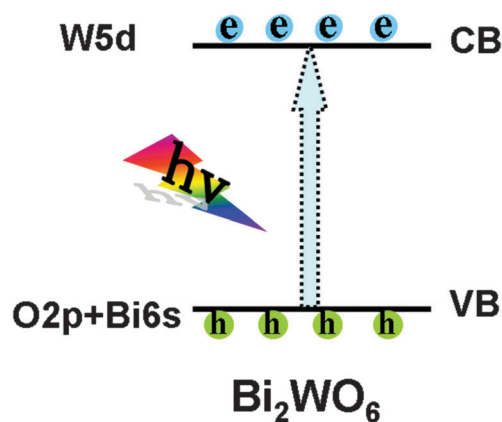


Fig. 1 Band structure of the Bi_2WO_6 photocatalyst.

Such band structure indicates that charge transfer in Bi_2WO_6 upon photoexcitation occurs from the $\text{O}2p+\text{Bi}6s$ hybrid orbitals to the empty $\text{W}5d$ orbitals, as illustrated in Fig. 1.

It is now accepted that the efficiency of the photocatalytic process is closely related to (i) the generation of photogenerated electron–hole pairs in the semiconductor photocatalysts, as well as to (ii) the separation and utilization of the charge carriers. Optimization of these two phenomena guides the exploration of visible light-driven photocatalysts.^{5–13,15–22,36–43,49–53,60–64,103–107} Furthermore, (iii) controllable morphology was proven to be an essential factor to tune the electronic structure of photocatalysts obviously playing an important role in determining the overall photoactivity.^{56,107–118} Over the past decade, great attention has been paid to Bi_2WO_6 -based photocatalysis, especially on tuning its nanostructure to optimize the photocatalytic performance.^{68–101} In 2005, Bi_2WO_6 nanoplates with square laminar morphologies (Fig. 2a–c) were synthesized by a simple hydrothermal method.⁷² As illustrated in Fig. 2d, the formation of tiny crystalline nuclei occurs firstly in a supersaturated medium. Then tiny crystalline nuclei made of orthorhombic Bi_2WO_6 crystals grow to form irregular particles at the expense of smaller particles due to their energy difference in solubility according to the Gibbs–Thomson law.⁷² As the reaction continues, irregular particles dissolve and a small laminar structure is formed which then develops into larger nanoplates due to anisotropic growth along the (001) plane parallel to the intrinsic layered structure.⁷² Eventually, larger nanoplates are formed.

This work offered the first case to synthesize Bi_2WO_6 nanostructure by a facile hydrothermal treatment,⁷² opening the route to the efficient fabrication of nano-architected Bi_2WO_6 . Afterwards indeed copious reports have been published that address new strategies to synthesize Bi_2WO_6 with specific configurations, including one-dimensional (1D) Bi_2WO_6 (nanofibers⁷³ and hollow tubes⁷⁴), two-dimensional (2D) Bi_2WO_6 (nanoplates⁹⁴ and microdiscs⁷⁵) and three-dimensional (3D) Bi_2WO_6 (flower-like,^{76,77,99,100} flake-ball,^{78,79} nest-like Bi_2WO_6 ,^{80,81} microspheres,^{82–85} nanocages,⁸⁷ hollow spheres,^{92,93,95} and inverse opals⁹⁶).

Among these Bi_2WO_6 structures, the 3D assemblies have received more attention because of their unique architecture and properties.^{68,70,71,76–85,87,91–93,95,96,99,100}

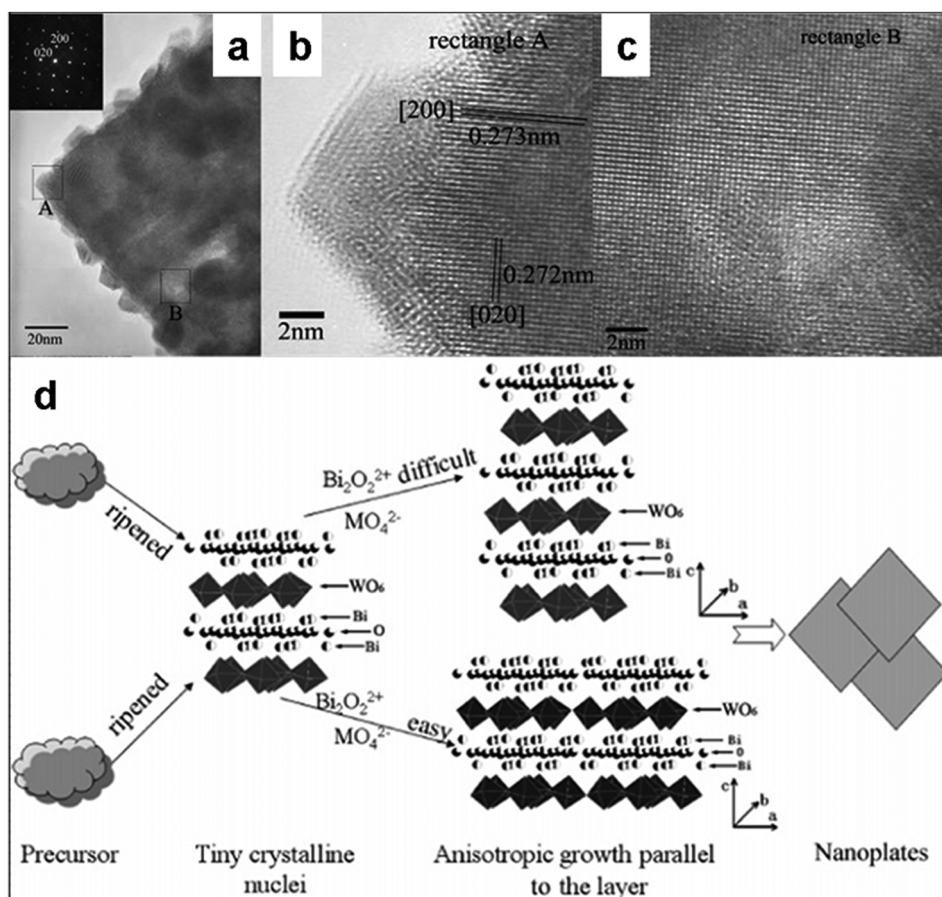


Fig. 2 (a) TEM image of the Bi_2WO_6 nanoplates. (b and c) HRTEM images of rectangle A and B in (a), respectively. (d) Anisotropic growth mechanism of Bi_2WO_6 nanoplates. Reprinted with permission from ref. 72. Copyright 2005 American Chemical Society.

Hydro/solvothermal treatment is a predominant approach to construct 3D-structured Bi_2WO_6 due to the ease of the experimental process and high efficiency.^{68,70,71,76,78–85,92,99,100} The formation of 3D Bi_2WO_6 assemblies obtained through the hydro/solvothermal reactions often consists of three main steps: (i) the formation of Bi_2WO_6 particles at the early stage, (ii) the development of 2D nanoplates through anisotropic growth and the Ostwald ripening process, and (iii) the organization of 3D Bi_2WO_6 structures from the corresponding 2D nanoplates.^{68,70,71,76,79,82,83,85,92}

For instance, Wang's group has reported a flower-like Bi_2WO_6 superstructure (Fig. 3a–c) synthesized by a facile hydrothermal process without any surfactant or template.⁷⁶ The formation mechanism is depicted in Fig. 3d, which offers a typical example for the fabrication of 3D Bi_2WO_6 *via* the three-step procedure mentioned above.⁷⁶

Thereafter, a series of 3D structured Bi_2WO_6 have been constructed by tuning the experimental parameters (*e.g.*, the precursor, reaction temperature, acidity of the medium, solvent or surfactant),^{77–85} which further enrich the Bi_2WO_6 structures' nanochemistry world.^{77–85}

In order to widen the potential applications of Bi_2WO_6 , hollow nanostructures and ordered array of Bi_2WO_6 have also been developed due to their attractive physical and chemical properties.^{74,86,87,91,92,96,97} The templating method is the classical

synthetic approach for hollow nanostructures and ordered arrays.^{86,87,91,96,97,119} In this regard, monodisperse silica spheres, polystyrene (PS) spheres and carbon spheres are often utilized as the hard templates due to their cost efficiency and easy manipulation.^{86,87,91,96,97} For example, Bi_2WO_6 nanocages have been successfully synthesized with colloidal carbon as the template by a refluxing process in ethylene glycol (EG), as shown in Fig. 4.⁸⁷

The use of EG could produce the complex of M (Bi^{3+} or WO_4^{2-}) with $-\text{OH}$ *via* coordination.⁸⁷ During the refluxing process, the complex gradually decomposes to release the metal ions, followed by the reaction for producing Bi_2WO_6 crystals. As a result, Bi_2WO_6 grains coated carbon spheres are formed. In the calcination process, Bi_2WO_6 nanoparticles grow from these small grains and the nanocages are formed as replicas of the carbon sphere.⁸⁷

Bi_2WO_6 arrays with the specific ordered structures have also been reported.^{96,97} Bahnemann and co-workers prepared Bi_2WO_6 inverse opals through the evaporation-induced self-assembly method, as illustrated in Fig. 5a.⁹⁶ The homogeneous amorphous complex was chosen as the precursor produced in aqueous solution by complexation between low-cost metal salts $\text{Bi}(\text{NO}_3)_3$ and $\text{H}_{26}\text{N}_6\text{O}_{41}\text{W}_{12}(x\text{H}_2\text{O})$ and diethylenetriaminepentaacetic acid (H_5DTPA). Starting from this complex precursor,

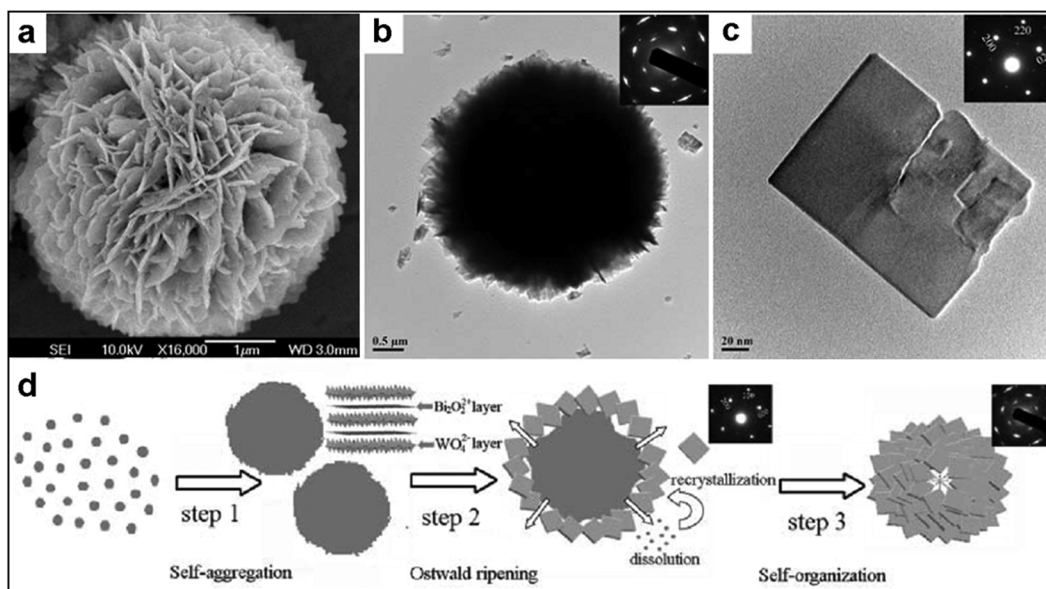


Fig. 3 (a) SEM, (b) TEM images of an individual flower-like Bi_2WO_6 sphere. (c) TEM image of a Bi_2WO_6 peeled fragment. (d) The formation mechanism of flower-like Bi_2WO_6 . Reprinted with permission from ref. 76. Copyright 2007 Royal Society of Chemistry.

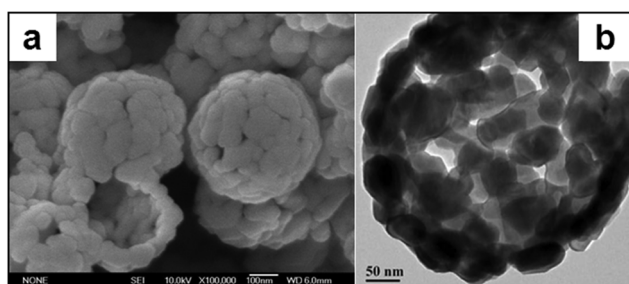


Fig. 4 (a) SEM and (b) TEM images of Bi_2WO_6 nanocages. Reprinted with permission from ref. 87. Copyright 2009 American Chemical Society.

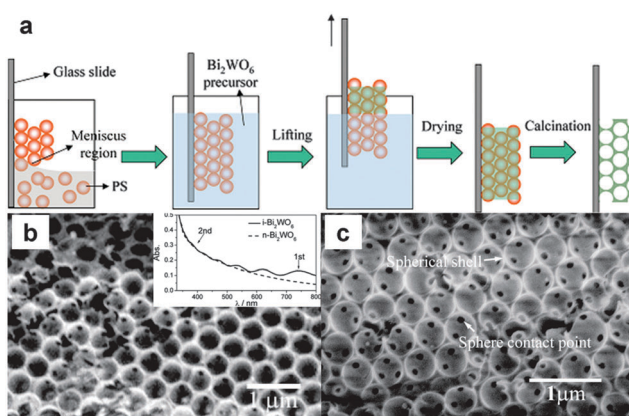


Fig. 5 (a) Schematic illustration of the preparation of Bi_2WO_6 inverse opals. (b and c) SEM images of Bi_2WO_6 inverse opals (inset of (b): the absorption spectra of Bi_2WO_6 inverse opals and a reference Bi_2WO_6 film). Reprinted with permission from ref. 96. Copyright 2011 Wiley-VCH.

crystallized Bi_2WO_6 with a pure phase can be obtained at relatively low temperature, thus avoiding the destruction of

the inverse-opal structure. As shown in Fig. 5b and c, Bi_2WO_6 inverse opals are easily obtained upon calcination removing the PS opal templates. Such Bi_2WO_6 inverse opals smartly integrate the merits of semiconductor Bi_2WO_6 and those of photonic crystals, including their optical and structural advantages for better performance.⁹⁶

Looking back to the development of Bi_2WO_6 structures from the earliest Bi_2WO_6 bulk powders produced by solid state reaction to 3D architectures or ordered arrays of Bi_2WO_6 ,^{66,68–101} we may realize that, owing to the evolution of nanomaterials,¹²⁰ more precise control of the Bi_2WO_6 structural and morphology configuration at the atomic scale was achieved. This enables us to tune the functional properties of Bi_2WO_6 for specific application, especially in the photocatalytic processes,^{66,68–101} as shown in the following sections.

3. Bi_2WO_6 nanostructures for selective organic synthesis

Although Bi_2WO_6 as a visible-light photocatalyst has been mainly utilized for non-selective degradation of organic pollutants or bacteria,^{68–93} recent reports demonstrate that applying nanostructured Bi_2WO_6 for selective organic transformations is a promising route for value-added chemical synthesis.^{99–101} Xu and co-workers lately discovered that flower-like Bi_2WO_6 can serve as a highly selective visible-light photocatalyst toward aerobic selective oxidation of glycerol, a renewable biomass chemical, to dihydroxyacetone (DHA) using oxygen as the unique oxidant in water at room temperature and atmospheric pressure.⁹⁹ The flower-like Bi_2WO_6 nanostructure obtained from 8 h hydrothermal treatment shows optimum visible light photoactivity in terms of glycerol conversion and DHA yield. The main byproduct is found to be glyceraldehyde. Time-online

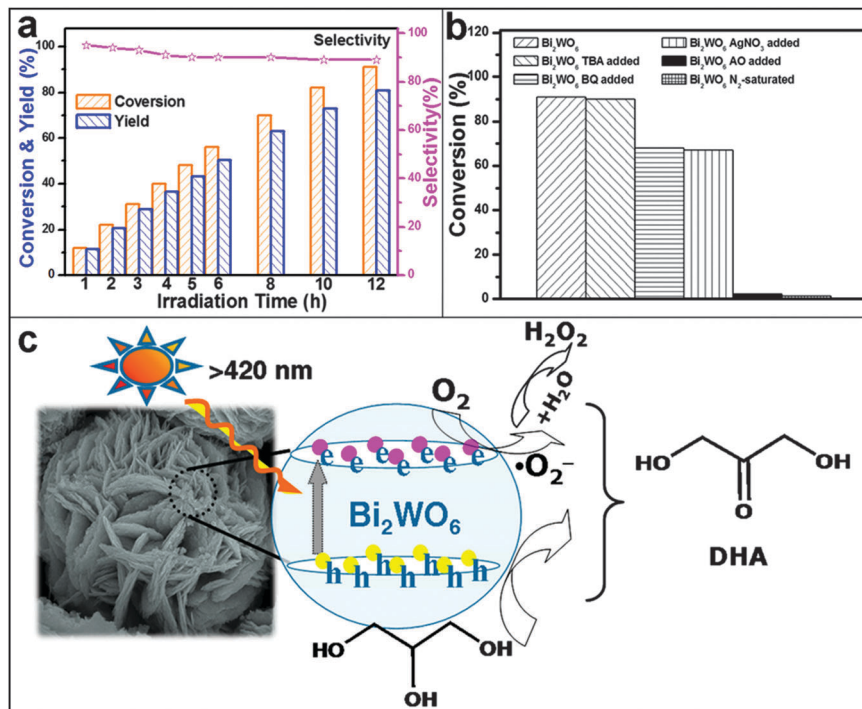


Fig. 6 (a) Time-online photoactivity, (b) controlled experiments under a N₂-saturated atmosphere and using different radical scavengers and (c) the proposed mechanism toward selective oxidation of glycerol to DHA in water over Bi₂WO₆ with the hydrothermal treatment for 8 h under visible light irradiation ($\lambda > 420$ nm). Reprinted with permission from ref. 99. Copyright 2013 Royal Society of Chemistry.

data in Fig. 6a reveal that the Bi₂WO₆ photocatalyst maintains its high selectivity to target product DHA at a high conversion with evolution of the reaction. In addition, DHA is easily desorbed from the surface of flower-like Bi₂WO₆, which is beneficial for obtaining high selectivity to the target product. The recycled activity tests indicate that the catalyst is stable towards aerobic oxidation of glycerol to DHA in water.

The cause and reaction mechanism for the high selectivity of DHA in water over Bi₂WO₆ under visible-light irradiation have been studied through a series of controlled experiments with radical scavengers and physico-chemical characterization.⁹⁹ Fig. 6c shows that electron-hole pairs are generated over Bi₂WO₆ under visible-light irradiation. The positive holes could oxidize the adsorbed glycerol on the surface of Bi₂WO₆ to the corresponding intermediate, which further reacts with oxygen or activated oxygen (e.g., O₂^{•-}) to produce the target product DHA. The non-selective hydroxyl ([•]OH) radicals are not involved in this photocatalytic oxidation process, as confirmed by the characterization analysis and by control experiments (Fig. 6b).⁹⁹

Inspired by the discovery of Bi₂WO₆ towards visible-light photocatalytic selective oxidation of glycerol,⁹⁹ more recently, Xu's group offered another evidence to further demonstrate the capability of the Bi₂WO₆ photocatalyst in the field of selective organic transformations induced by visible-light illumination.¹⁰⁰ The team found that benzylic alcohols can be oxidized to the corresponding aldehydes with high selectivity in water over flower-like Bi₂WO₆ using oxygen as an oxidant under mild conditions.¹⁰⁰ Also in this case, the highly chemoselective photocatalytic performance of Bi₂WO₆ toward oxidation of benzylic alcohols in water can be attributed to the mild

oxidation power of Bi₂WO₆, the absence of hydroxyl radicals, and the weaker adsorption capacity of aldehydes compared to alcohols over the flower-like Bi₂WO₆.¹⁰⁰

Overall, these findings encouragingly demonstrate the wide scope and potential of the Bi₂WO₆ photocatalyst for chemical synthesis.^{99,100} Together our groups recently reported a simple and feasible sol-gel encapsulation method to directly transform flower-like Bi₂WO₆ into an entrapped sol-gel leach-proof photocatalyst (Fig. 7) of enhanced activity, named SiliaSun.¹⁰¹

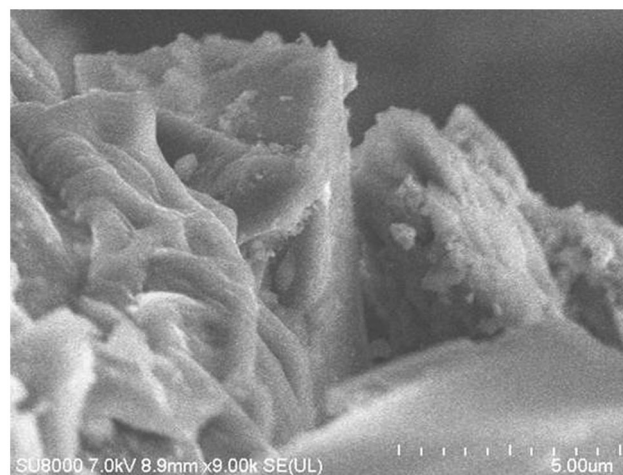
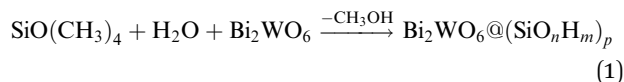


Fig. 7 SEM picture of the silica-entrapped Bi₂WO₆ (the weight content of Bi₂WO₆ is 10%). Reprinted with permission from ref. 101. Copyright 2014 Royal Society of Chemistry.

When such a nanochemistry strategy is applied (eqn (1)), the visible-light photoactivity of Bi_2WO_6 toward aerobic selective conversion of glycerol to related products (*i.e.*, dihydroxyacetone and glyceraldehydes) in water is greatly enhanced, while the high selectivity is retained. The results suggest that, even using 0.4 mg or 0.8 mg of visible-light-photoactive Bi_2WO_6 , the conversion of glycerol over SiliaSun after 4 h of visible-light irradiation is 2–3 times higher than that over 8 mg of non-entrapped Bi_2WO_6 .^{99,101}



The sol–gel silica encapsulation was found to contribute to the improved separation of photogenerated electron–hole pairs from Bi_2WO_6 , as well as to the increased specific surface area with significant specific pore volume and thus to the enhanced adsorption capacity toward glycerol.^{99,101} Besides, the synergy between the silica matrix and photoactive entrapped Bi_2WO_6 allows the tuneable control of both activity and selectivity for photocatalytic oxidation of glycerol under visible-light irradiation, enabling a catalytic process capable of affording valued products at low cost with little or no waste generation.¹⁰¹

These results^{99–101} highlight the great potential of semiconductor Bi_2WO_6 with a specific nano-architecture in photocatalytic selective organic synthesis in water under mild conditions, which represents a typical tenet of green and sustainable chemistry. In particular, the versatile nanochemistry of Bi_2WO_6 strongly suggests that there is a wide scope to advance the application of nanostructured Bi_2WO_6 in the field of photocatalytic selective organic redox reactions for the synthesis of value-added chemicals, instead of being stuck in the field of non-selective degradation processes.^{66,68–101} In brief, progress achieved in this area may pave the way toward new efficient Bi_2WO_6 -based photocatalytic systems for organic transformations for the green synthesis of a wide variety of chemicals.

4. Bi_2WO_6 nanostructures to make fuels from CO_2 and H_2O

The aggravating energy issues require mankind to turn to renewable and clean solar energy for making fuels. On the other hand, the combustion of coal and hydrocarbons greatly increases the concentration of CO_2 in the atmosphere and leads to the formation of fine particulate matter, which is polluting the air of large regions of the world. In this regard, the efficient photocatalytic conversion of CO_2 into valuable solar fuels such as methane or methanol might address future energy supply demand and mitigate CO_2 emissions.⁸ Hitherto, two pioneering discoveries using photoactive Bi_2WO_6 to make fuels have been reported.^{94,95}

In 2011, Zou and co-workers reported a remarkable increase in the CO_2 reduction with water to yield CH_4 over Bi_2WO_6 square nanoplates (Fig. 8a–c) under visible-light irradiation as compared to yield over Bi_2WO_6 made by solid state reaction (SSR).⁹⁴ In detail, the CH_4 production rate increases from $0.045 \mu\text{mol g}^{-1} \text{h}^{-1}$ for the SSR sample to $1.1 \mu\text{mol g}^{-1} \text{h}^{-1}$ for the nanoplate catalyst (Fig. 8d).⁹⁴

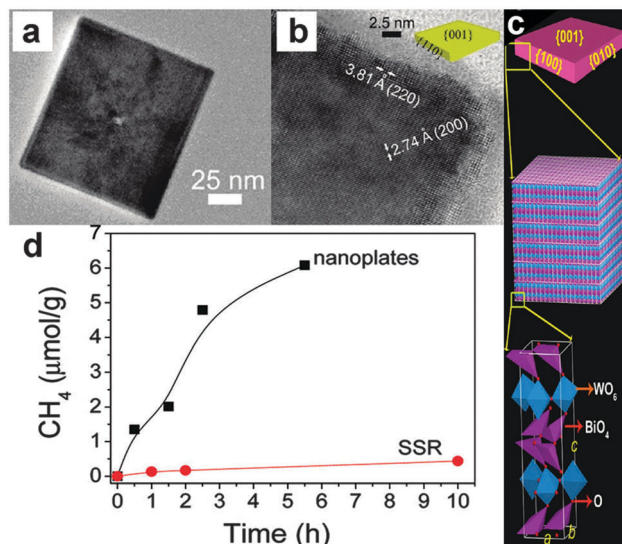


Fig. 8 (a) TEM, (b) HRTEM and (c) structural model of Bi_2WO_6 square nanoplates. (d) CH_4 generation over nanoplates and the SSR sample under visible-light irradiation ($\lambda > 420 \text{ nm}$). Reprinted with permission from ref. 94. Copyright 2011 American Chemical Society.

Considering that the band gap of Bi_2WO_6 nanoplates is very close to that of the SSR sample, the photoactivity enhancement should mainly be ascribed to geometrical factors. Firstly, reducing the nanoplate lateral dimension to the nanometer length scale offers a higher specific surface area. Secondly, the ultrathin geometry of the nanoplate enhances the charge carrier mobility from the bulk onto the surface where they participate in the photoreduction reaction. Thirdly, the preferentially exposed (001) crystal plane of the nanoplates is more effective than other crystal planes.⁹⁴

In 2012, Huang and co-workers synthesized Bi_2WO_6 hollow microspheres (HMSs) *via* an anion exchange strategy based on the Kirkendall effect and utilized it for photocatalytic reduction of CO_2 to methanol.⁹⁵ Such HMSs afford a $32.6 \mu\text{mol g}^{-1}$ of methanol formation yield, which is 25.5 times higher than that ($1.28 \mu\text{mol g}^{-1}$) of bulk Bi_2WO_6 prepared by solid state reaction under the same conditions. Again, this enhancement was attributed to the hierarchical hollow architectures endowed by Bi_2WO_6 hollow microspheres with more surface active sites and better morphology for the same spacial charge transfer from the bulk of the nanocrystals to the surface.⁹⁵ In addition, Bi_2WO_6 HMSs display no photoactivity decrease in the recycling experiments. This work shows that hierarchical inorganic materials with hollow interiors may provide a generalized design strategy to achieve better photocatalytic efficiency of CO_2 conversion by microstructure modulation.

From a practical viewpoint, the optimization of the reaction system is required, especially in the adsorption capacity for CO_2 of the photocatalyst and in the availability of the photogenerated charge carriers for reaction, prior to quenching of electrons and holes at the material's outer surface. Finally, to close the materials cycle, atmospheric CO_2 easily fixed and desorbed using diamine-functionalized silica gel¹²¹ will be utilized to photocatalytically convert it into fuels, methanol or methane.

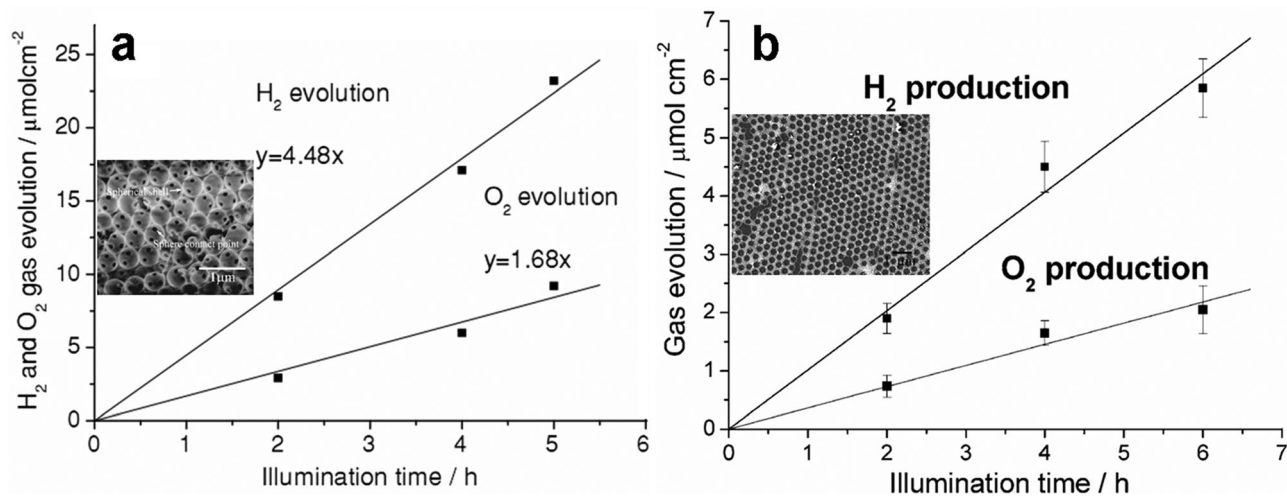


Fig. 9 H₂ and O₂ evolution on (a) the Bi₂WO₆ inverse opal electrode with an external potential of 0.8 V and (b) the Bi₂WO₆ 2D array photoanode at a potential of 0.4 V vs. Ag/AgCl under visible-light irradiation ($\lambda > 400$ nm). The insets are the corresponding SEM images. Reprinted with permission from ref. 96 and 97. Copyright 2011 and 2013 Wiley-VCH.

Photocatalytic water splitting into hydrogen and oxygen is perhaps the most important goal of contemporary research in chemistry aimed to alleviate the energy and environmental crises. Although the reduction potential of electrons in Bi₂WO₆ is not sufficient to reduce H⁺ to obtain H₂,^{66,72,89,90} three recent studies clearly showed that photocatalytic water splitting on Bi₂WO₆ can be achieved by applying an external potential to produce clean solar hydrogen.^{96–98} Bi₂WO₆ inverse opals used as photoanodes, for instance, are effective in photoelectrochemical water splitting.⁹⁶ Results in Fig. 9a show that the evolution rate of H₂ is 4.5 $\mu\text{mol h}^{-1} \text{cm}^{-2}$. The measured anodic photocurrent is 0.25 mA cm^{-2} , from which a theoretical H₂ evolution rate of 4.7 $\mu\text{mol h}^{-1} \text{cm}^{-2}$ is derived. This result indicates that the photocurrent is almost entirely employed for water splitting. Such a phenomenon has also been observed for the Bi₂WO₆ 2D ordered arrays prepared by a simple self-assembly procedure.⁹⁷ As compared to the conventional photoanode with similar thickness, the Bi₂WO₆ 2D array photoanode exhibits a much higher photocurrent density and photon-to-H₂ conversion efficiency even with a small amount of Bi₂WO₆ (Fig. 9b). This can be ascribed to the superior light scattering, more efficient photogenerated hole diffusion and larger surface area of the Bi₂WO₆ 2D array structure.⁹⁷ Furthermore, the photocurrent and morphology of the Bi₂WO₆ electrode are stable under the working conditions employed by the team,⁹⁷ which is obviously crucial from the application viewpoint.

Finally, in 2012 Amal and co-workers developed a Bi₂WO₆ film *via* transforming anodized WO₃ film into Bi₂WO₆ by substituting the intercalated water molecules with [Bi₂O₂]²⁺ in a hydrothermal treatment.⁹⁸ The resultant Bi₂WO₆ film is readily used as an electrode to produce anodic photocurrent and H₂ evolution on the Pt counter electrode under visible light irradiation.⁹⁸ When an applied voltage of 1.0 V *versus* Pt (two-electrode system) is applied, the H₂ gas evolution rate remains approximately constant at 0.1 $\mu\text{mol h}^{-1}$ within the first 4 h of visible-light illumination.

These preliminary results definitely corroborate the feasibility of the Bi₂WO₆ photocatalyst for hydrogen evolution under visible-light irradiation with an external potential.^{96–98} Although its photon energy conversion is not at the stage of practical use, the potential of this technology for producing a clean fuel as solar hydrogen¹⁰⁶ is great in view of three aspects. Firstly, the faradaic efficiency using a Bi₂WO₆ photoanode can reach *ca.* 100%; that is, the photocurrent is almost completely employed for hydrogen production. Secondly, there is wide room to optimize the efficiency of Bi₂WO₆ for making fuels by nanochemistry methods to tune the material's nanostructure and morphology. Thirdly, the photoelectrochemical activity of Bi₂WO₆ can be further improved by modification or doping strategies of the Bi₂WO₆ photoanode, in addition to the electrode architecture construction.

5. Outlook and conclusions

“Given the difficulties associated with homogeneous routes employed so far for artificial photosynthesis”, wrote Bard in 1995, “heterogeneous arrays will be needed for high-efficiency solar energy conversion, with new semiconductor materials and multielectron catalysts likely to emerge as key components of such heterogeneous arrays, perhaps with small metal clusters or films to protect the semiconductor surface”.¹⁵ Twenty years later new semiconductor materials and heterogenization strategies are indeed leading to promising results. New semiconductor materials such as Bi₂WO₆ are used to overcome some of the practical barriers encountered in attempts to utilize the solar spectrum,^{66,68–101} while heterogenization *via* sol-gel encapsulation in highly porous silica has opened the route to both highly stable photosynthetic bioreactors² and visible-light photocatalysts for selective organic synthesis.¹⁰¹ The transparency, stabilization and high surface area of the silica matrix allow light penetration, promote the separation efficiency of

the photogenerated electron–hole pairs and drastically enhance adsorption capacity toward the substrate. Control of the sol–gel cage, namely of the confined nanoenvironment surrounding the entrapped photoactive species, can tune the efficiency and selectivity of the photocatalyst, making a truly green chemical process possible.¹⁰¹

As emphasized by Steinfeld,¹²² efficiency concerns the economy of processes, and thus industry. Sustainability, however, is about closing the energy and material cycles. Hence, if the use of renewable solar energy closes the energy cycle, the use of renewable carbon feedstock is required to make chemical synthetic processes truly sustainable. In this respect, the highly selective processes, during which bioglycerol, alcohols, atmospheric CO₂ and water are turned into fine chemicals and fuels over Bi₂WO₆ nanostructures, are truly promising. The latest advances in this field mostly rely on developing various techniques for fabricating nanostructured Bi₂WO₆ photocatalysts.^{94–101} In other words, the nanochemistry strategies used to make photoactive Bi₂WO₆ nanostructures with specific architectures or with sol–gel encapsulation allow us to extend the application of nanostructured Bi₂WO₆-based photocatalysts to organic synthesis and fuel production.

Although well-developed Bi₂WO₆-based photocatalytic systems remain scanty, and controllability of these systems is expected to be further improved for practical applications, research in this area is clearly progressing. Studies on Bi₂WO₆ photocatalysis began only a decade ago, namely nearly three decades after the 1972 discovery of TiO₂ electrodes for photocatalytic water splitting under UV light irradiation.^{4,66} The much younger field of visible-light Bi₂WO₆ photocatalysis may learn some appropriate approaches from ultraviolet-light TiO₂ catalysis.¹²³ The development of TiO₂ photocatalysts from fundamental studies to practical application indeed provides inspiration for the community to steer and promote the advances of Bi₂WO₆ visible-light photocatalyst systems. For example, nanostructured Bi₂WO₆ with specific morphology or an exposed crystalline plane has been fabricated to increase the surface area and enhance the photocatalytic activity.^{68,70–73,86,89,94} Moreover, hierarchical Bi₂WO₆ has also been developed to combine the advantages of high photocatalytic performance from nanostructures with easy recycling of hierarchical architectures, moving Bi₂WO₆ photocatalysis closer to applicability to commercial processes.^{68,70,71,76,79,80,84,87,95,99,100}

In most applications of TiO₂ photocatalysis, fixed-bed reactor configurations with immobilized particles or semiconductor ceramic membranes are employed.⁵ In the typical fixed-bed photocatalytic reactor, the photocatalyst is coated on the walls of a solid-supported matrix, or around the casing of the light source.¹²⁴ However, the most notable drawback of these reactors is the low surface area-to-volume ratio.⁵ Photochemistry practitioners recently emphasized¹²⁵ that, in order to find application in organic synthesis, photocatalytic syntheses must be intensified through the use of large area photo-reactors under flow in which the photons acting as reagents are introduced as a stream (flux), so that the flow rate can be precisely tailored to match the photon stream and the quantum yield of the substrate. In this respect, the sol–gel approach holds great promise for better utilization of the Bi₂WO₆ semiconductor in synthetic organic chemistry.

In the late 1980s, the broad photochemistry of sol–gel doped glasses was pioneered by Avnir and co-workers.¹²⁶ The application of those achievements has mainly been confined to develop highly sensitive sol–gel sensors and biosensors,¹²⁷ many of which are now commercialized, and protective optical coatings.¹²⁸ Now, the sol–gel entrapment methodology can be extended to develop cost-effective and highly selective heterogeneous photocatalysis for organic synthesis. Straightforward deposition of sol–gel entrapped nanostructured bismuth tungstate as a thin film over the inner surface of the tube macroflow photoreactor will afford the required high productivities while working under visible-light irradiation, avoiding altogether the use of ultraviolet-light.

The resulting doped sol–gel glasses show long-term chemical and physical stability, while low cost and easily made Bi₂WO₆ nanostructures make the case for economically viable processes. Followed by Mexico, China (6500 tonnes out of 8900 tonnes mining production in the world in 2010) is the major producer of mined bismuth.¹²⁹ In addition, bismuth, a metal element with unusually low toxicity, is obtained as a byproduct of extraction of other metals, such as lead, copper, tin, molybdenum and tungsten.¹³⁰ The incremental annual production of bismuth throughout the past century indicates the sustainability of its production.¹³¹ Tungsten is abundant and low cost (currently 45 USD kg^{−1}) with China mining nearly 85% of the tungsten globally mined in 2012.¹³²

Under such circumstances, there are good reasons to be optimistic that Bi₂WO₆-based photocatalyst systems will become increasingly useful for making chemicals and clean fuels, eventually finding widespread application. Along with developments in nanoscience and technology, numerous opportunities will emerge to enhance our capability to advance semiconductor photocatalysts into a versatile and powerful tool for wide applications in chemical synthesis and fuel production beyond we have realized to date. We envisage a not too distant future in which sol–gel entrapped Bi₂WO₆ will be expanded from basic science to make valued chemicals in photoreactors working under ultramild conditions. Eventually many commercially relevant reactions for the synthesis of valued chemicals from biomass, as well as fuels from carbon dioxide and water, will be carried out in similar photoreactors providing a powerful chemical tool contributing to make the realization of Ciamician's dream closer.

Acknowledgements

This article is dedicated to University of Palermo's Dr Mauro Agate for many years of friendship with one of us. The support by the NSFC (21173045, 20903023), the Award Program for Minjiang Scholar Professorship, the NSF of Fujian Province for Distinguished Young Investigator Grant (2012J06003), and Program for Returned High-Level Overseas Chinese Scholars of Fujian Province is gratefully acknowledged.

References

- 1 G. Ciamician, *Science*, 1912, **36**, 385–394.
- 2 C. F. Meunier, P. Dandoy and B.-L. Su, *J. Colloid Interface Sci.*, 2010, **342**, 211–224.

- 3 G. P. Peters, R. M. Andrew, T. Boden, J. G. Canadell, P. Ciais, C. Le Quere, G. Marland, M. R. Raupach and C. Wilson, *Nat. Clim. Change*, 2013, **3**, 4–6.
- 4 A. Fujishima and K. Honda, *Nature*, 1972, **238**, 37–38.
- 5 M. R. Hoffmann, S. T. Martin, W. Choi and D. W. Bahnemann, *Chem. Rev.*, 1995, **95**, 69–96.
- 6 F. Wen and C. Li, *Acc. Chem. Res.*, 2013, **46**, 2355–2364.
- 7 Q. Xiang, J. Yu and M. Jaroniec, *Chem. Soc. Rev.*, 2012, **41**, 782–796.
- 8 M.-Q. Yang and Y.-J. Xu, *Phys. Chem. Chem. Phys.*, 2013, **15**, 19102–19118.
- 9 G. Palmisano, V. Augugliaro, M. Pagliaro and L. Palmisano, *Chem. Commun.*, 2007, 3425–3437.
- 10 N. Zhang, Y. Zhang and Y.-J. Xu, *Nanoscale*, 2012, **4**, 5792–5813.
- 11 A. Maldotti, A. Molinari and R. Amadelli, *Chem. Rev.*, 2002, **102**, 3811–3836.
- 12 N. Zhang, S. Liu and Y.-J. Xu, *Nanoscale*, 2012, **4**, 2227–2238.
- 13 M. A. Fox and M. T. Dulay, *Chem. Rev.*, 1993, **93**, 341–357.
- 14 V. Augugliaro, V. Loddo, M. Pagliaro, G. Palmisano and L. Palmisano, *Clean by Light Irradiation*, RSC Publishing, Cambridge, 2010.
- 15 A. J. Bard and M. A. Fox, *Acc. Chem. Res.*, 1995, **28**, 141–145.
- 16 A. B. Murphy, P. R. F. Barnes, L. K. Randeniya, I. C. Plumb, I. E. Grey, M. D. Horne and J. A. Glasscock, *Int. J. Hydrogen Energy*, 2006, **31**, 1999–2017.
- 17 F. Andrew Frame, E. C. Carroll, D. S. Larsen, M. Sarahan, N. D. Browning and F. E. Osterloh, *Chem. Commun.*, 2008, 2206–2208.
- 18 T. Uchihara, M. Matsumura, J. Ono and H. Tsubomura, *J. Phys. Chem.*, 1990, **94**, 415–418.
- 19 G. Chandra De, A. M. Roy and S. S. Bhattacharya, *Int. J. Hydrogen Energy*, 1996, **21**, 19–23.
- 20 A. W. H. Mau, C. B. Huang, N. Kakuta, A. J. Bard, A. Campion, M. A. Fox, J. M. White and S. E. Webber, *J. Am. Chem. Soc.*, 1984, **106**, 6537–6542.
- 21 M.-Q. Yang, B. Weng and Y.-J. Xu, *J. Mater. Chem. A*, 2014, **2**, 1710–1720.
- 22 B. Weng, S. Liu, N. Zhang, Z.-R. Tang and Y.-J. Xu, *J. Catal.*, 2014, **309**, 146–155.
- 23 D. S. Bhachu, S. Sathasivam, C. J. Carmalt and I. P. Parkin, *Langmuir*, 2013, **30**, 624–630.
- 24 N. Zhang, J. Shi, S. S. Mao and L. Guo, *Chem. Commun.*, 2014, **50**, 2002–2004.
- 25 J. Krishna Reddy, B. Srinivas, V. Durga Kumari and M. Subrahmanyam, *ChemCatChem*, 2009, **1**, 492–496.
- 26 J. Bandara, U. Klehm and J. Kiwi, *Appl. Catal., B*, 2007, **76**, 73–81.
- 27 K. J. Kim and Y. R. Park, *Solid State Commun.*, 2003, **127**, 25–28.
- 28 T. Ohmori, H. Takahashi, H. Mametsuka and E. Suzuki, *Phys. Chem. Chem. Phys.*, 2000, **2**, 3519–3522.
- 29 L. Zhang, W. Wang, J. Yang, Z. Chen, W. Zhang, L. Zhou and S. Liu, *Appl. Catal., A*, 2006, **308**, 105–110.
- 30 D. Meissner, R. Memming and B. Kastening, *J. Phys. Chem.*, 1988, **92**, 3476–3483.
- 31 R. M. Cornell and U. Schwertmann, *The Iron Oxides*, Wiley-VCH Verlag GmbH & Co. KGaA, Weinheim, 1996.
- 32 M. Woodhouse and B. A. Parkinson, *Chem. Mater.*, 2008, **20**, 2495–2502.
- 33 F. J. Morin, *Phys. Rev.*, 1954, **93**, 1195–1199.
- 34 A. Walsh and G. W. Watson, *J. Solid State Chem.*, 2005, **178**, 1422–1428.
- 35 G. W. Watson, S. C. Parker and G. Kresse, *Phys. Rev. B: Condens. Matter Mater. Phys.*, 1999, **59**, 8481–8486.
- 36 Y. I. Kim, S. J. Atherton, E. S. Brigham and T. E. Mallouk, *J. Phys. Chem.*, 1993, **97**, 11802–11810.
- 37 Z. Zou, J. Ye, K. Sayama and H. Arakawa, *Nature*, 2001, **414**, 625–627.
- 38 H. Yamashita, M. Harada, J. Misaka, M. Takeuchi, K. Ikeue and M. Anpo, *J. Photochem. Photobiol., A*, 2002, **148**, 257–261.
- 39 S. U. M. Khan, M. Al-Shahry and W. B. Ingler, *Science*, 2002, **297**, 2243–2245.
- 40 S. Sakthivel and H. Kisch, *Angew. Chem., Int. Ed.*, 2003, **42**, 4908–4911.
- 41 R. Asahi, T. Morikawa, T. Ohwaki, K. Aoki and Y. Taga, *Science*, 2001, **293**, 269–271.
- 42 J. C. Yu, W. Ho, J. Yu, H. Yip, P. K. Wong and J. Zhao, *Environ. Sci. Technol.*, 2005, **39**, 1175–1179.
- 43 G. Hitoki, T. Takata, J. N. Kondo, M. Hara, H. Kobayashi and K. Domen, *Chem. Commun.*, 2002, 1698–1699.
- 44 B. Ohtani, H. Osaki, S. Nishimoto and T. Kagiya, *J. Am. Chem. Soc.*, 1986, **108**, 308–310.
- 45 Y. Mao and A. Bakac, *J. Phys. Chem.*, 1996, **100**, 4219–4223.
- 46 H. Sun, F. Blatter and H. Frei, *J. Am. Chem. Soc.*, 1996, **118**, 6873–6879.
- 47 M. A. Fox and M. J. Chen, *J. Am. Chem. Soc.*, 1983, **105**, 4497–4499.
- 48 S. Yurdakal, G. Palmisano, V. Loddo, V. Augugliaro and L. Palmisano, *J. Am. Chem. Soc.*, 2008, **130**, 1568–1569.
- 49 N. Zhang, M.-Q. Yang, Z.-R. Tang and Y.-J. Xu, *ACS Nano*, 2014, **8**, 623–633.
- 50 M. A. Fox, *Acc. Chem. Res.*, 1983, **16**, 314–321.
- 51 Y. Zhang, Z.-R. Tang, X. Fu and Y.-J. Xu, *ACS Nano*, 2011, **5**, 7426–7435.
- 52 I. Izumi, W. W. Dunn, K. O. Wilbourn, F.-R. F. Fan and A. J. Bard, *J. Phys. Chem.*, 1980, **84**, 3207–3210.
- 53 M.-Q. Yang, Y. Zhang, N. Zhang, Z.-R. Tang and Y.-J. Xu, *Sci. Rep.*, 2013, **3**, 3314.
- 54 S. Yurdakal, G. Palmisano, V. Loddo, O. Alagoz, V. Augugliaro and L. Palmisano, *Green Chem.*, 2009, **11**, 510–516.
- 55 M. Cherevatskaya, M. Neumann, S. Földner, C. Harlander, S. Kümmel, S. Dankesreiter, A. Pfitzner, K. Zeitler and B. König, *Angew. Chem., Int. Ed.*, 2012, **51**, 4062–4066.
- 56 Y. Zhang, N. Zhang, Z.-R. Tang and Y.-J. Xu, *ACS Sustainable Chem. Eng.*, 2013, **1**, 1258–1266.
- 57 G. Palmisano, M. Addamo, V. Augugliaro, C. Tullio, E. García-López, V. Loddo and L. Palmisano, *Chem. Commun.*, 2006, 1012–1014.
- 58 N. Zhang, Y. Zhang, M.-Q. Yang, Z.-R. Tang and Y.-J. Xu, *J. Catal.*, 2013, **299**, 210–221.

- 59 T. J. Jacobsson, V. Fjallstrom, M. Sahlberg, M. Edoff and T. Edvinsson, *Energy Environ. Sci.*, 2013, **6**, 3676–3683.
- 60 A. Iwase, Y. H. Ng, Y. Ishiguro, A. Kudo and R. Amal, *J. Am. Chem. Soc.*, 2011, **133**, 11054–11057.
- 61 Q. Xiang, J. Yu and M. Jaroniec, *J. Am. Chem. Soc.*, 2012, **134**, 6575–6578.
- 62 A. Primo, T. Marino, A. Corma, R. Molinari and H. García, *J. Am. Chem. Soc.*, 2011, **133**, 6930–6933.
- 63 K. Maeda, M. Higashi, D. Lu, R. Abe and K. Domen, *J. Am. Chem. Soc.*, 2010, **132**, 5858–5868.
- 64 K. Maeda and K. Domen, *J. Phys. Chem. Lett.*, 2010, **1**, 2655–2661.
- 65 W. J. Youngblood, S.-H. A. Lee, K. Maeda and T. E. Mallouk, *Acc. Chem. Res.*, 2009, **42**, 1966–1973.
- 66 A. Kudo and S. Hijii, *Chem. Lett.*, 1999, 1103–1104.
- 67 H. G. Kim, D. W. Hwang and J. S. Lee, *J. Am. Chem. Soc.*, 2004, **126**, 8912–8913.
- 68 L. Zhang, H. Wang, Z. Chen, P. K. Wong and J. Liu, *Appl. Catal., B*, 2011, **106**, 1–13 and references therein.
- 69 S.-H. Chen, Z. Yin, S.-L. Luo, X.-J. Li, L.-X. Yang and F. Deng, *Appl. Surf. Sci.*, 2012, **259**, 7–12.
- 70 L. Zhang and Y. Zhu, *Catal. Sci. Technol.*, 2012, **2**, 694–706 and references therein.
- 71 Y. Feng, Q. Wu, G. Zhang and Y. Sun, *Prog. Chem.*, 2012, **24**, 2124–2131 and references therein.
- 72 C. Zhang and Y. Zhu, *Chem. Mater.*, 2005, **17**, 3537–3545.
- 73 M. Shang, W. Wang, J. Ren, S. Sun, L. Wang and L. Zhang, *J. Mater. Chem.*, 2009, **19**, 6213–6218.
- 74 S.-J. Liu, Y.-F. Hou, S.-L. Zheng, Y. Zhang and Y. Wang, *CrystEngComm*, 2013, **15**, 4124–4130.
- 75 X. Wang, L. Chang, J. Wang, N. Song, H. Liu and X. Wan, *Appl. Surf. Sci.*, 2013, **270**, 685–689.
- 76 L. Zhang, W. Wang, Z. Chen, L. Zhou, H. Xu and W. Zhu, *J. Mater. Chem.*, 2007, **17**, 2526–2532.
- 77 X.-F. Cao, L. Zhang, X.-T. Chen and Z.-L. Xue, *CrystEngComm*, 2011, **13**, 306–311.
- 78 F. Amano, K. Nogami, R. Abe and B. Ohtani, *Chem. Lett.*, 2007, **36**, 1314–1315.
- 79 F. Amano, K. Nogami, R. Abe and B. Ohtani, *J. Phys. Chem. C*, 2008, **112**, 9320–9326.
- 80 J. Wu, F. Duan, Y. Zheng and Y. Xie, *J. Phys. Chem. C*, 2007, **111**, 12866–12871.
- 81 L. Xu, X. Yang, Z. Zhai and W. Hou, *CrystEngComm*, 2011, **13**, 7267–7275.
- 82 D. He, L. Wang, H. Li, T. Yan, D. Wang and T. Xie, *CrystEngComm*, 2011, **13**, 4053–4059.
- 83 Z. Chen, L. Qian, J. Zhu, Y. Yuan and X. Qian, *CrystEngComm*, 2010, **12**, 2100–2106.
- 84 D. Ma, S. Huang, W. Chen, S. Hu, F. Shi and K. Fan, *J. Phys. Chem. C*, 2009, **113**, 4369–4374.
- 85 Y. Li, J. Liu, X. Huang and G. Li, *Cryst. Growth Des.*, 2007, **7**, 1350–1355.
- 86 L.-W. Zhang, Y.-J. Wang, H.-Y. Cheng, W.-Q. Yao and Y.-F. Zhu, *Adv. Mater.*, 2009, **21**, 1286–1290.
- 87 M. Shang, W. Wang and H. Xu, *Cryst. Growth Des.*, 2009, **9**, 991–996.
- 88 H. Xie, D. Shen, X. Wang and G. Shen, *Mater. Chem. Phys.*, 2007, **103**, 334–339.
- 89 H. Fu, C. Pan, W. Yao and Y. Zhu, *J. Phys. Chem. B*, 2005, **109**, 22432–22439.
- 90 J. Tang, Z. Zou and J. Ye, *Catal. Lett.*, 2004, **92**, 53–56.
- 91 S. Sun, W. Wang and L. Zhang, *J. Mater. Chem.*, 2012, **22**, 19244–19249.
- 92 X.-J. Dai, Y.-S. Luo, W.-D. Zhang and S.-Y. Fu, *Dalton Trans.*, 2010, **39**, 3426–3432.
- 93 D. Wu, H. Zhu, C. Zhang and L. Chen, *Chem. Commun.*, 2010, **46**, 7250–7252.
- 94 Y. Zhou, Z. Tian, Z. Zhao, Q. Liu, J. Kou, X. Chen, J. Gao, S. Yan and Z. Zou, *ACS Appl. Mater. Interfaces*, 2011, **3**, 3594–3601.
- 95 H. Cheng, B. Huang, Y. Liu, Z. Wang, X. Qin, X. Zhang and Y. Dai, *Chem. Commun.*, 2012, **48**, 9729–9731.
- 96 L. Zhang, C. Baumanis, L. Robben, T. Kandiel and D. Bahnemann, *Small*, 2011, **7**, 2714–2720.
- 97 L. Zhang and D. Bahnemann, *ChemSusChem*, 2013, **6**, 283–290.
- 98 C. Ng, A. Iwase, Y. H. Ng and R. Amal, *J. Phys. Chem. Lett.*, 2012, **3**, 913–918.
- 99 Y. Zhang, N. Zhang, Z.-R. Tang and Y.-J. Xu, *Chem. Sci.*, 2013, **4**, 1820–1824.
- 100 Y. Zhang and Y.-J. Xu, *RSC Adv.*, 2014, **4**, 2904–2910.
- 101 Y. Zhang, R. Ciriminna, G. Palmisano, Y.-J. Xu and M. Pagliaro, *RSC Adv.*, 2014, **4**, 18341–18346.
- 102 M. Pagliaro, *Glycerol: The Platform Biochemical of the Chemical Industry*, Simplicissimus Book Farm, Milan, 2013.
- 103 Y. Zhang, N. Zhang, Z.-R. Tang and Y.-J. Xu, *Phys. Chem. Chem. Phys.*, 2012, **14**, 9167–9175.
- 104 Y.-J. Xu, Y. Zhuang and X. Fu, *J. Phys. Chem. C*, 2010, **114**, 2669–2676.
- 105 A. Ishikawa, T. Takata, J. N. Kondo, M. Hara, H. Kobayashi and K. Domen, *J. Am. Chem. Soc.*, 2002, **124**, 13547–13553.
- 106 M. Pagliaro, A. G. Konstandopoulos, R. Ciriminna and G. Palmisano, *Energy Environ. Sci.*, 2010, **3**, 279–287.
- 107 Y. Zhang, N. Zhang, Z.-R. Tang and Y.-J. Xu, *Chem. Sci.*, 2012, **3**, 2812–2822.
- 108 Z.-R. Tang, F. Li, Y. Zhang, X. Fu and Y.-J. Xu, *J. Phys. Chem. C*, 2011, **115**, 7880–7886.
- 109 P. Li, Z. Wei, T. Wu, Q. Peng and Y. Li, *J. Am. Chem. Soc.*, 2011, **133**, 5660–5663.
- 110 F. Lu, W. Cai and Y. Zhang, *Adv. Funct. Mater.*, 2008, **18**, 1047–1056.
- 111 S. Yanagida, M. Kanemoto, K.-i. Ishihara, Y. Wada, T. Sakata and H. Mori, *Bull. Chem. Soc. Jpn.*, 1997, **70**, 2063–2070.
- 112 F. Amano, K. Nogami and B. Ohtani, *J. Phys. Chem. C*, 2009, **113**, 1536–1542.
- 113 Y. B. Chen, L. Z. Wang, G. Q. Lu, X. D. Yao and L. J. Guo, *J. Mater. Chem.*, 2011, **21**, 5134–5141.
- 114 N. Zhang, X. Fu and Y.-J. Xu, *J. Mater. Chem.*, 2011, **21**, 8152–8158.
- 115 H. Tong, S. Ouyang, Y. Bi, N. Umezawa, M. Oshikiri and J. Ye, *Adv. Mater.*, 2011, **24**, 229–251.

- 116 T. R. Gordon, M. Cargnello, T. Paik, F. Mangolini, R. T. Weber, P. Fornasiero and C. B. Murray, *J. Am. Chem. Soc.*, 2012, **134**, 6751–6761.
- 117 N. Zhang, S. Liu, X. Fu and Y.-J. Xu, *J. Phys. Chem. C*, 2011, **115**, 22901–22909.
- 118 I. S. Cho, M. Logar, C. H. Lee, L. Cai, F. B. Prinz and X. Zheng, *Nano Lett.*, 2014, **14**, 24–31.
- 119 N. Zhang and Y.-J. Xu, *Chem. Mater.*, 2013, **25**, 1979–1988.
- 120 H. C. Zeng, *Acc. Chem. Res.*, 2013, **46**, 226–235.
- 121 J. A. Wurzbacher, C. Gebald and A. Steinfeld, *Energy Environ. Sci.*, 2011, **4**, 3584–3592.
- 122 A. Steinfeld, Sun New Energy Conference, RSC Publishing, S. Flavia, Italy, 2012.
- 123 Y. Wang, H.-X. Lin, L. Chen, S.-Y. Ding, Z.-C. Lei, D.-Y. Liu, X.-Y. Cao, H.-J. Liang, Y.-B. Jiang and Z.-Q. Tian, *Chem. Soc. Rev.*, 2014, **43**, 399–411.
- 124 D. W. Bahnemann, D. Bockelmann, R. Goslich, M. Hilgendorff and D. Weichgrebe, *Photocatalytic Purification and Treatment of Water and Air*, Elsevier, Amsterdam, 1993.
- 125 J. P. Knowles, L. D. Elliott and K. I. Booker-Milburn, *Beilstein J. Org. Chem.*, 2012, **8**, 2025–2052.
- 126 A. Slama-Schwok, D. Avnir and M. Ottolenghi, *Photochem. Photobiol.*, 1991, **54**, 525–534.
- 127 B. Dunn and J. I. Zink, *J. Mater. Chem.*, 1991, **1**, 903–913.
- 128 H. Cui, M. Zayat, P. G. Parejo and D. Levy, *Adv. Mater.*, 2008, **20**, 65–68.
- 129 United States Geological Survey, Bismuth Statistics and Information, <http://minerals.usgs.gov/minerals/pubs/commodity/bismuth/>, last time accessed November 20, 2013.
- 130 J. Krüger, P. Winkler, E. Lüderitz, M. Lück and H. U. Wolf, *Ullmann's Encyclopedia of Industrial Chemistry*, Wiley-VCH Verlag GmbH & Co. KGaA, Weinheim, 2003.
- 131 United States Geological Survey, Bismuth Statistics and Information, <http://minerals.usgs.gov/minerals/pubs/commodity/bismuth/>, Minerals Yearbook.
- 132 United States Geological Survey, Tungsten Statistics and Information, <http://minerals.usgs.gov/minerals/pubs/commodity/tungsten/>, last time accessed November 20, 2013.